JOURNAL OF MATERIALS SCIENCE: MATERIALS IN MEDICINE **16** (2005) 807–819

Osteogenic differentiation of mesenchymal progenitor cells in computer designed fibrin-polymer-ceramic scaffolds manufactured by fused deposition modeling

JAN-THORSTEN SCHANTZ[1,2,*], ARTHUR BRANDWOOD[5], DIETMAR WERNER HUTMACHER[1,3], HWEI LING KHOR[1,4], KATHARINA BITTNER[6]
[1]*Division of Bioengineering,* [2]*Division of Plastic Surgery,* [3]*Department of Orthopedic Surgery,* [4]*Department of Material Science, National University of Singapore, Singapore*
E-mail: surjts@nus.edu.sg
[5]*Graduate School of Biomedical Engineering, University of New South Wales, Sydney, Australia*
[6]*Baxter Biosurgery, Munich, Germany*

Biomimetic scaffolds offer great potentials in the development of bone analogs for tissue engineering. The studies presented in this paper focus specifically on the osteogenic potential of the novel PCL/CaP matrices and its degradation behavior. Biodegradable Polymer-ceramic Scaffolds were fabricated using the solid free form fabrication technology: Fused Deposition Modeling (FDM). The scaffold architecture was characterized by a honeycomb-like design and a complete interconnectivity of the pores. Human mesenchymal stem cells (MSCs) were seeded together with fibrin glue into PCL/CaP scaffolds and cultured *in vitro* for periods of up to eight weeks. Cellular adhesion, proliferation and osteogenic differentiation were assessed in these constructs using a range of histological and microscopic techniques. In additional experiments, degradation was assessed by measuring mass loss, diameter change, molecular weight change and by scanning electron micrographs. MSCs were able to adhere, migrate, and differentiate along the osteogenic lineage with in these scaffolds. The PCL/CaP scaffolds showed up to 27 fold increased degradation of compared to PCL scaffolds.

Abbreviations

2D,3D	Two Dimensional, Three dimensional
DAPI	4.6-diamidino-2-phenylindol
CaP	Calcium Phosphate
CLM	Confocal Laser Microscopy
ECM	Extra Cellular Matrix
EDAX	Energy Dispersive X-Ray Analysis
EYFP	Enhanced Yellow Fluorescence Protein
FDA	Fluorescein Diacetate
FDM	Fused Deposition Modeling
FITC	Fluorescein isothiocyanate
GPC	Gel Permeation Chromatography
LSAB	Labeled Streptavidin Biotin
PCL-CaP	Polycaprolactone Calcium Phosphate
MSC	Mesenchymal Stem Cell
PBS	Phosphate-buffered saline
PCL	Polycaprolactone
PI	Propidium Iodide
PLGA	poly(L)glycolide
PDLA	poly(D)lactide
PLLA	poly(L)lactide
SEM	Scanning Electron Microscopy
SFF	Sold Free Form

1. Introduction

The requirements for production of an effective tissue engineering construct are (1) ease of manufacture of a scaffold with appropriate geometry; (2) successful *in vitro* culture in which cells proliferate sufficiently and differentiate into appropriate cell types with appropriate phenotypic expression and (3) control of seeding and distribution of these cells and other components within the scaffold to produce the final construct [1, 2].

Following implant these scaffold/cell constructs must stimulate organization into the appropriate tissue structure while possessing adequate mechanical integrity to provide sufficient mechanical support prior to

*Author to whom all correspondence should be addressed.

establishment of repaired tissue. Finally the degradation rate of the scaffold must be attuned to the repair and remodeling process so that sufficient strength and stiffness is maintained as a gradual transfer of mechanical support takes place from the scaffold to the strengthening, maturing tissue.

Successful scaffold designs are likely to require precise control over morphology and structure to optimize requirements for mechanical properties, mass transfer, cell seeding and accommodation of remodeling [1, 3, 4]. Bulk preparation methods (essentially production of foams by methods such as salt leaching or use of gaseous blowing agents) can exert only general controls over the material structure in terms of overall levels of porosity or pore sizes. In order to produce scaffolds of more precisely defined structures, researchers have turned to solid free form (SFF) manufacturing techniques which allow reproducible, computerized design and manufacture of precisely defined three dimensional (3D) architectures [5, 6].

Based on the concept of biomimetics to provide a matrix which mimics structural and compositional characteristics of bone tissue, researchers have also explored production of composite scaffolds containing additives such as calcium phosphates, designed to modify cell differentiation or remodeling processes [7–9]. Solid Free Form techniques also provide opportunities for more precise control of distribution of materials components in composite scaffolds.

In this paper we report *in vitro* studies on tissue engineering constructs prepared, using fused deposition modeling (FDM), from poly-ε-caprolactone (PCL) with potentially osteoconductive enhancement of addition of micro particulate calcium phosphate ceramic (CaP) to the synthetic polymer matrix and by use of fibrin glue as a physiologic extra cellular matrix (ECM) to control and improve the cell seeding process and the proliferation in culture.

PCL has previously been shown to support cell attachment and proliferation of osteoblast-like cells and has been investigated as a matrix material for craniofacial reconstruction [10–12]. We have previously described tissue engineering constructs using PCL scaffolds which provide suitable mechanical properties for load bearing applications in bone reconstruction and which can be rapidly and easily manufactured in a wide range of shapes and controlled microstructures using FDM [1]. These scaffolds have been shown to direct the three-dimensional arrangement of seeded osteoblast-like cells, so that mineralized tissue structures are formed throughout the entire scaffold architecture [13].

Osteoconductive effects of Calcium phosphates are well documented [8, 14–17] including a number of approaches involving compounding various calcium phosphate ceramics into the polymer matrix of scaffolds [18]. Mikos and co-workers have been investigating multi-layer composite tricalciumphosphate materials for osseous reconstruction [19–20]. However, most of the conventional scaffold techniques have the disadvantage that the compounded ceramic particulate tends to be separated from direct cell contact by a skin of polymer at the matrix surface [6].

In contrast SFF manufacturing procedures allow the incorporation of CaP in the form of micro particulates which are exposed on the scaffold surfaces [1, 13]. Therefore it would be expected that the presence of CaP in direct cell and/or tissue contact will render the materials more osteoconductive, promoting higher rates of cell attachment, proliferation and differentiation into mineralizing tissue. Furthermore, the addition of CaP has been shown [3, 21, 22] to produce a buffering effect, preventing local acidification caused by high localized concentrations of acidic byproducts from too rapid a degradation process and avoiding associated adverse tissue responses.

It may also be expected that buffering effects would modify the degradation kinetics and allow some control over degradation rate by variation of the amount of added CaP. Therefore the degradation behavior of these constructs was investigated by *in vitro* accelerated testing.

Seeding of cells onto scaffolds using conventional aqueous media is problematic in that the effects of gravity and flow during the seeding process cause inefficient seeding (30–70% of cells can be lost depending on scaffold morphology) and uneven distribution of cells in the construct, [23–25]. This effect is especially critical in SFF and textile-based scaffolds. It has been shown that suspension of the cells in a hydrogel, such as fibrin glue, provides greater control of the seeding process and produces a higher density, more uniform seeding which in turn would be expected to produce a more uniform and complete osteogenesis [13, 26–27]. Furthermore, the development and normal functioning of osteogenic cells depends on interactions with molecules in their immediate micro-environment. The extracellular matrix (ECM) includes a number of different macromolecules whose structural integrity and functional composition are important in maintaining normal tissue architecture and function. The ECM exerts influence on behavior (adherence-spreading-migration-differentiation) of cells. Fibrin is an important component of ECM, especially in healing tissue, and the use of fibrin gel as a cell support permits the development of a model system which mimics physiologically relevant *in vivo* conditions.

In this paper we present cell culture studies which characterize the osteogenic potential of the PCL-CaP/hMSC-fibrin constructs *in vitro* in order to assess their suitability for bone tissue engineering applications, plus an accelerated degradation study to determine the degradation and resorption kinetics of FDM manufactured PCL-CaP scaffolds.

2. Materials and methods

2.1. Scaffold design, fabrication and characterization

2.1.1. Compounding of PCL-CaP

PCL powder (catalog no. 44,074-4 Aldrich Chemical Company, Inc., Milwaukee, Wisconsin), M_n of ca. 80,000 Dalton (GPC) and melt index of 1.0 g/10 min (125 °C/44psi ASTM D1238-73) and Hydroxyapatite (microemulsion derived CaP powder) were dried

separately for 24 h in a vacuum oven at 120 and 40 °C, respectively. Composite pellets of PCL-CaP were then formed by casting a solvent mixture of 20 g PCL/CaP blend with 25 wt% content CaP. The composite material was cut into 0.5 × 0.5 cm pellets and stored in a dessicator until used. The PCL-CaP pellets were melt-extruded to form monofilaments (1.6 + 0.1 mm) using a one-shot extruder (Alex James & Associates Inc., Greensville, SC).

3D scaffolds were then fabricated as sheets of 50 × 50 × 3 mm from the PCL powder and from PCL-CaP monofilaments by fused deposition modeling using an FDM 3D Modeler rapid prototyping system (Stratasys, Eden Prairie, MN). Based on keying the design parameters in the QuickSlice Software scaffolds with layers of neatly aligned filaments with a diameter of 0.25 mm and a gap of 0.50 mm between filaments. The scaffolds were designed with a lay-down pattern of 0/60/120 °.

Scaffolds cylinders of diameter of 6 mm and height of 3 mm were punched out (using a disposable biopsy punch, Miltex, Lake Success, NY) from the rectangular sheets produced by the FDM machine.

2.1.2. Surface and 3D morphology

To assess the matrix morphology and distribution of the CaP within the scaffold and on the surface, samples of finished scaffolds were imaged using Micro Computed Tomography, using the methods of Lin *et al*. [28] and Scanning electron microscopy (JEOL JSM-5600LV at accelerating voltage of 15 mV under low vacuum).

2.2. Degradation study

Scaffold cylinders were soaked in 5 M sodium hydroxide for different time periods as shown in Table I. Five replicates were used for each time period and material. After the allotted time period, samples were removed and the degradation process halted by rinsing thoroughly with de-ionized water until the water did not feel soapy, showing that sodium hydroxide was thoroughly washed off.

2.2.1. Mass loss and diameter change

Degraded samples were dried in a vacuum oven at 35 °C for four hours (determined in separate trials to be sufficient time to dry to constant mass) Fiber diameter was then measured using a micro-screw meter; scanning electron microscope and optical microscope were used to monitor diameter of PCL-HA fibers (they were too soft to be measured using the micro-screw meter).

2.2.2. Molecular weight

Molecular weight was determined by Gel permeation chromatography (Waters 2690 Separation Module using 2 columns Waters Styragel HR4E and HR5E.) The polymers were dissolved in tetrahydrofuran. The PCL and PCL-HA samples were left in the solvent on a shaker for 1 day and filtered with a 0.2 μm inorganic membrane filter.

TABLE I Time frame of degradation study

Material	Time (days)
PCL fibers	1, 4, 10, 18
PCL-CaP fibers	1, 4, 6, 8

2.3. Isolation and characterization of human bone marrow derived stem cells

Bone marrow (∼10) was aspirated from the iliac crest of a patient who underwent reconstructive surgery. The marrow was immediately diluted with 2 times volume of heparinised saline solution (50 IU Heparin in 5 ml Pharmacia Upjohn) to prevent initial clotting. Human mesenchymal stem cells (hMSCs) were isolated from the bone marrow aspirate by density gradient centrifugation.

Osteogenic differentiation was assessed by staining with Alizarin Red to visualize mineralization. Adherent cells were amplified in monolayer culture using MesenCult H5400 stem cell medium supplemented with 10% FBS (Stem Cell Technologies Inc., Vancouver, BC, Canada), 1% HEPES Buffer and 1% Penicillin/Streptomycin (all Gibco, Invitrogen, Grand Island, NY). Initial absence of osteoblastic phenotype expression of precursor cells was confirmed by Osteocalcin and Alkaline Phosphatase antibody staining. To induce osteogenic differentiation the standard medium was supplemented with osteogenic supplements (ascorbic acid, β glycerol phosphate and dexamethasone). Cells were fixed with 4% paraformaldehyde and stained with 1% Alizarin-Red S solution in water for 10 min and then viewed under standard light microscopy.

To characterise the morphology and the proliferative characteristics of the isolated MSC's deriving from fibroblast-like colonies in the early phase of cell culture a colony forming unit fibroblast assay CFU-F was performed. Cells were incubated at 37 °C, 5% CO_2 for 14 days. At the end of the culture period the medium was removed and residual non-adherent cells removed by washing with phosphate buffered saline ph 7.4 (PBS). The adherent colonies were fixed with methanol then stained with Wright's Giemsa (Sigma, St. Louis, Miss) and examined by optical microscopy.

2.4. Seeding and culture of MSC within the scaffolds

After primary culture the cells were subsequently amplified and passage 4 cells were used for the seeding into the PCL-CaP scaffolds. Prior to seeding the scaffolds were treated 1 hour with NAOH as described previously [5] and then sterilized by centrifuging in 70% ethanol for 30 min at 1000 rpm. Then they were rinsed 3× in changes of PBS placed into 6 well TCPS cell culture plates and left in the incubator at 5% CO_2, 37 °C overnight for drying. Passage four MSCs were enzymatically lifted from T 150 polystyrene culture flasks with 0.25 trypsin/EDTA (Hyclone, Logan, Utah) and counted using a hemocytometer. Cell viability was assessed via trypan blue staining.

Cells were resuspended in medium and 3×10^5 cells were mixed with fibrinogen solution (Tisseel, Baxter Hyland Immuno, Vienna, Austria) at a ratio of 3:1 v/v and seeded by pippeting 80 μL of cell/fibrinogen mixture into PCL-CaP scaffolds. After seeding, 20 μL thrombin solution (Tisseel, Baxter Hyland-Immuno) diluted 1:2 with PBS was pipetted onto each scaffold to achieve fibrin polymerization resulting in a semi-rigid, homogeneously distributed, three-dimensional network within the scaffold architecture.

Constructs were transferred into 24 well plates and placed into the incubator at 5% CO_2, 37 °C, for 30 min to allow the fibrin glue-cell suspension to polymerize before they were carefully topped-up with 1 ml of culture medium. On day 3, osteoinduction was performed by adding induction medium I (MesenCult H5400, Vancouver BC) supplemented with 2 mM L-glutamine, 20% FBS, 1% Pen/Strep, 5×10^5 M beta-mercaptoethanol, 100 μM ascorbate-2-phosphate. After 7 days induction medium II (MesenCult H5400) supplemented with 10% FBS, 10% Pen/Strep, 25 mM Hepes, 100 μM ascorbic 2 phosphate, 1.8 mM KH_2PO_4, 10^{-8} M dexamethasone (Sigma, St. Louis, Miss) was exchanged for the first medium. Tissue constructs were kept in static culture conditions for up to 8 weeks with medium changed every 3rd day.

2.4.1. Cell metabolic activity assay

In order to assess cell proliferation in seeded constructs, an MTS assay of cell metabolic activity was performed (CellTiter 96^{TM} Aqueous One Solution Cell Proliferation Assay, Promega Corp. Madison, WI). PCL-CaP seeded constructs were assayed after 3 days and 2, 4, 6 and 8 weeks in culture as follows. Medium was removed from the wells and replaced with 500 μl of FBS-free culture medium. 100 μl MTS reagent was then to each well) and the plates incubated for 3 hrs (37 °C, 5% CO_2). Medium in each well was then mixed with a pipette to ensure homogeneity and 5×100 ul aliquots were pipetted from each well into a 96-well culture plate. Cell growth was determined by measuring the absorbance at 490 nm with a reference filter set at 620 nm in a plate reader (Microplate reader, Anthos HT III). The mean of the 5 readings was taken for each well/time point. Background absorbance was corrected by assaying control wells containing medium and PCL-CaP scaffolds only and calculating an average absorbance across all time points. Corrected absorbances at each time point were obtained by subtracting the background from the experimental results.

2.4.2. Cell morphology and adhesion analysis

To assess cellular adhesion and distribution within the scaffolds during the early culture phase and after 4 and 8 weeks in the culture, constructs were observed by confocal laser microscopy (CLM) and Scanning Electron Microscopy (SEM).

For CLM studies, seeded constructs were prepared by staining viable cells with the fluorescent dye Fluorescein Diacetate (FDA, Molecular Probes Inc., Eugene, Oregon) by incubation at 37 °C with 2 μg/ml FDA in PBS for 15 min. After rinsing twice in PBS, each sample was then placed in 0.1 mg/ml Propidium Iodide solution (PI, Molecular Probes, Oregon) for 5 mins at room temperature to stain dead cells red. The samples were then rinsed twice in PBS and viewed under an inverted Confocal Laser Microscope (Olympus IX 70 Fluoview HL SH 100, Olympus, Tokyo, Japan). Depth projection images were constructed from up to 25 horizontal image sections through the cultures.

For the characterization of cell spreading and cytoskeletal organization during cell adhesion to 2D and 3D substrata, the cells were transfected with EYFP-Tubulin (pEYFP Tubulin Vector, Clontech, Palo Alto, CA). Passage 4 cells were plated at a density of 70% in serum-free medium (Opti-MEM, Gibco, Invitrogen, Grand Island, NY) into Ø 20 cm polystyrene Petri dishes. Transfection was carried out as recommended from the manufacturer's protocol (Transfast, Promega, Madison, WI). Transfected cells were then plated onto glass cover slips (2D) or seeded into the PCL-CaP scaffolds (3D). After 24 h cytoskeletal structure was visualized using CLM by observing the EYFP fluorescence at an emission maximum of 527nm and an excitation maximum of 514 nm.

For SEM, 4 and 8 week samples were fixed for 20 min in 2.5% glutaraldehyde in 0.15M PBS, pH 1 7.4, dehydrated in graded ethanol series and gold sputtered prior to observation. Mounted samples were viewed under a Philips XL 30 FEG scanning electron microscope at an accelerating voltage of 5 kV.

2.4.3. Assessment of mineralisation by surface analysis

Assessment of mineralisation of the adhered cell layer was performed via energy dispersive X-ray analysis (EDAX) after 4 and 8 weeks in culture. The samples were fixed for 20 min with 2.5% glutaraldehyde in 0.15 M PBS (pH = 7.4) and dehydrated in increasing concentrations of ethanol. Qualitative and quantitative microanalytic analysis of the surface atoms was performed by detecting transmitted X-ray photons. The Calcium, Phosphorous and Sulphur ratio was determined in different regions of the sample using an EDAX CDU LEAP detector connected to a Philips XL 30 FEG scanning electron microscope (Phillips, Eindhoven, Netherlands). All samples were analyzed at a constant voltage of 20 kV under the same microscopical conditions. To assess Calcium and Phosphorus deposition, changes in the Calcium phosphate ratio between 4 and 8 weeks were compared by unpaired, two-tailed *t* tests. The results are expressed as means $\pm$ standard deviations, and considered as statistically significant of p was <0.05.

2.4.4. Cell differentiation

Differentiation of the MSCs into the osteogenic lineage was assessed by assay for expression of osteocalcin and collagen I. Constructs were fixed after 4 and 8 weeks in 4% paraformaldehyde for 10 min, washed in PBS, and

then embedded in tissue freezing medium (Jung, Nussloch, Germany). Cryosections (7 μm) were cut for immunohistochemical and immunofluorescence staining.

To demonstrate the osteogenic differentiation of the cells, the bone specific matrix protein osteocalcin was determined after 4 and 8 weeks in culture. Sections were treated with 0.2% Triton X to permeabilize cell membranes, then incubated for 30 min with 5% normal goat serum (Gibco, Invitrogen, Grand Island NY) to block nonspecific reactions, rinsed in PBS for 10 min and then incubated with the primary antibody (mouse anti-human Osteocalcin OC1 1:30, Biodesign, Saco, Maine) for 2 h at room temperature. Following 3 washes in PBS primary antibody sites were labeled with a fluorescein-conjugated secondary antibody for 1 h (FITC 1:64 anti mouse IgG fab-specific, Sigma Aldrich, St. Louis, Miss). Finally, cell nuclei were labeled with 4 μm/ml propidium-iodide-PBS for 5min and sections were mounted (DAKO Ultramount aqueous permanent mounting media, Carpinteria, CA) and observed using an Olympus IX 70 Confocal microscope.

2.4.5. Assessment of mineralization and calcified nodule formation

For extracellular matrix analysis, sections were incubated for 30 min at room temperature with primary antibodies against human Collagen I (1:20) (Southern Biotech Associates, Birmingham, Al). Binding sites were visualized using a labeled streptavidin biotin (LSAB) detection system (DAKO LSAB + Kit, Peroxidase Carpinteria, CA,). Counterstaining was performed with Gill's Haematoxylin (Sigma, St. Louis Miss).

Mineralisation of the ECM was assessed by visualization of nodules by Alizarine Complexone staining. After 4 and 8 weeks in culture, samples were fixed for 10 min in 3.7 w/v paraformaldehyde and sectioned into 10 μm slices with a Cryotome (Leica Bensheim Germany). The specimens were stained with the calcium specific dye, Alizarin-complexone *p*H7.2 (Sigma-Aldrich Chemical, St. Louis, Miss) for 10 min at room temperature. Nuclei were counter-stained with 4.6-diamidino-2-phenylindole (DAPI, 25 μg/ml Sigma Aldrich, St. Louis, Miss) for 15 min. Samples were mounted (DAKO, Ultramount aqueous permanent mounting media, Carpinteria, CA) and observed under fluorescence microscopy (Leica DM RXA, Bensheim, Germany).

3. Results

3.1. Scaffold characterization

3.1.1. Micro CT and SEM

The micro-CT data (Fig. 1(a)) show the gross scaffold morphology and cross sectional view of the

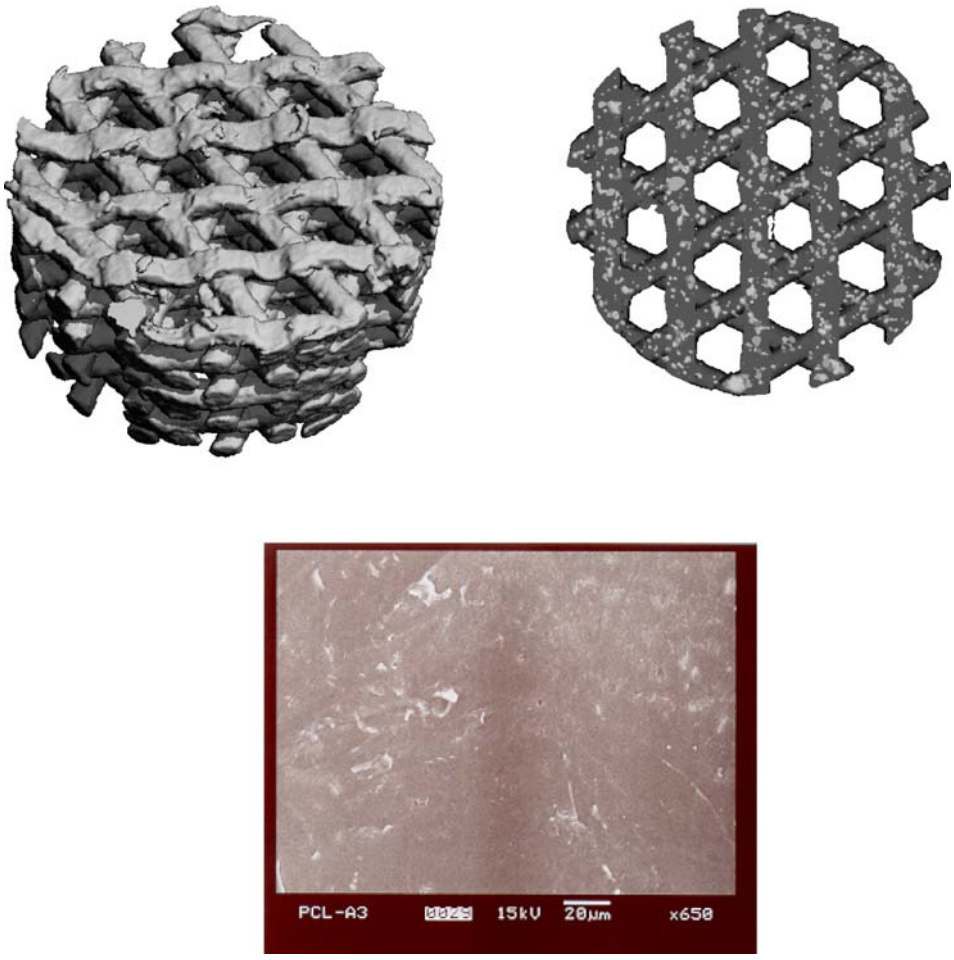

Figure 1 PCL-CaP scaffold architecture observed under micro computed tomography and scanning electron microscopy. An overview is shown in Fig. 1(a) and a cross-sectional view is given in Fig. 1(b). The distribution of the CaP granules within the polymer bars is indicated by the light grey areas (arrows). The scaffolds have a completely interconnected porous network. The SEM image (1c) shows the grainy surface morphology as a result of exposed CaP particles.

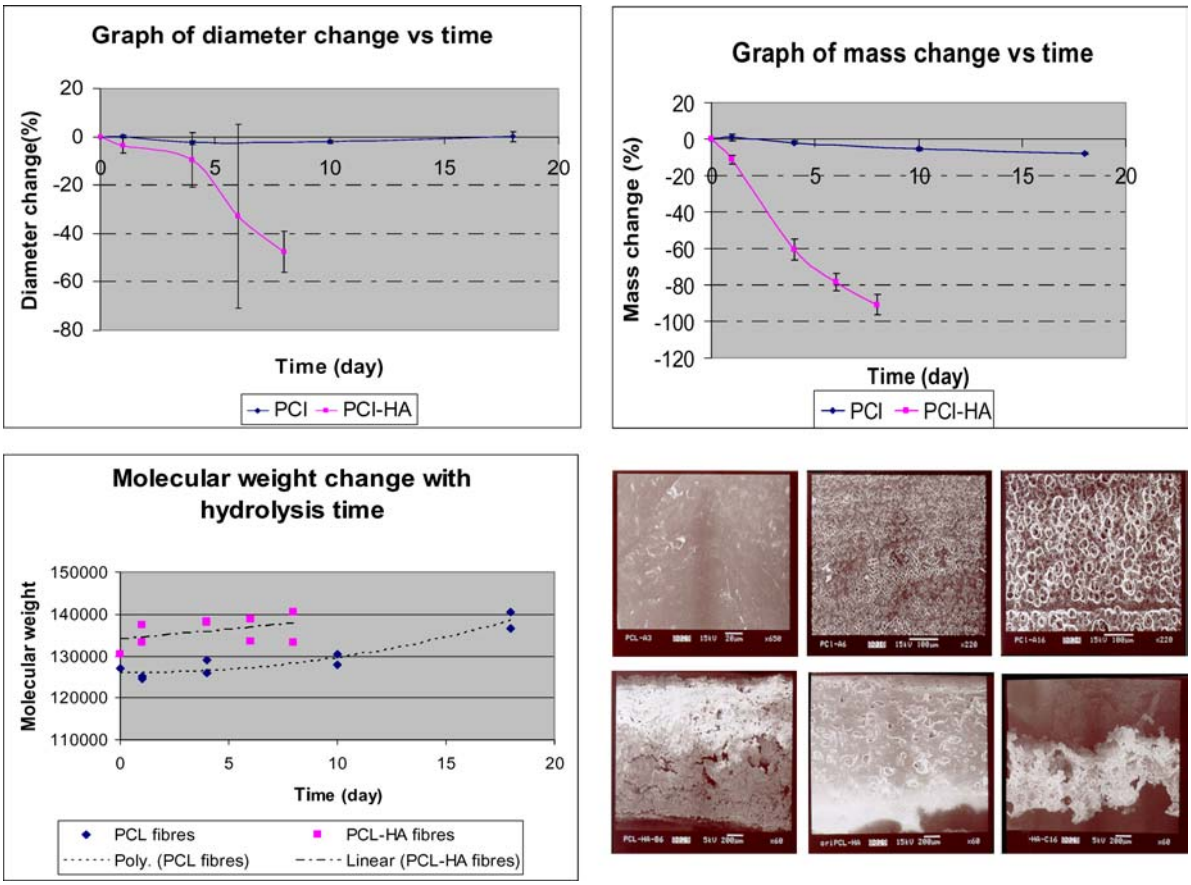

Figure 2 Diameter, mass and weight average molecular weight change of PCL and PCL-HA fibers with respect to degradation time is shown in Fig. 2(a)–(c) respectively. Scanning electron micrographs (2d) showing progressive surface topograhy change of PCL fibers (top row) and PCL-HA fibers (bottom row) due to hydrolytic degradation. Increasing degradation time increased size of pits on the surface of PCL fibers (top row). Evidence of macro-cracks, signs of bulk degradation of PCL-HA fibers (bottom row) observed after 4 days.

composite. The PCL-CaP scaffolds fabricated by FDM have a uniform reproducible bar architecture and interconnected pores in the size range 300–500 μm. The incorporated CaP particles are exposed and lead to a surface roughness on the bars of the material as shown by the SEM image (Fig. 1(c)). Within the bars the CaP particles appeared uniformly distributed (Fig. 1(b)).

3.2. Degradation

The mass loss pattern and SEM examination of the accelerated degradation test (Fig. 2) showed that PCL and PCL-CaP mainly degrade via surface erosion. The composite material with a 20% CaP composition degrades approximately 27 times faster than the PCL.

3.3. Isolation and characterization of human bone marrow derived stem cells

In the CFU-F assay, MSCs formed colonies visible at the 3rd day in culture. The number of colonies increased progressively to a maximum at days 7–10. Thereafter, only the size of the colonies increased. The colonies presented two main morphologies: (1) large spindle shaped cells that formed circular dense colonies. (2) Large flat cells present within these colonies were characterized by a large nucleus with multiple vacuoles in the cytoplasm Fig. 3(a) shows a stained culture dish after 14 days of incubation. Fig. 3(b) shows phase contrast photomicrographs of Wright's Giemsa stained isolated colonies after 14 days in culture. The rate of proliferation of the two cell populations was extremely variable. The large cells did not form colonies and multiplied significantly slower then the fibroblast-like cells. Upon osteogenic induction the MSC produce extracellular matrix in the form of mineralized nodules which were detected via Alizarin Red S stain (Fig. 3(c)).

3.4. Seeding and culture of MSC within the scaffolds

3.4.1. Cell morphology and adhesion analysis

Fig. 4(a)–(e) Shows analysis of cell adhesion, proliferation and differentiation on the PCL/CaP-fibrin scaffolds. The left panel shows schematically the process, the right panel depicts phase contrast light microscopy pictures.

The formation of focal adhesion is visualized using confocal laser microscopy and scanning electron microscopy (Fig. 5(a)–(d)). For up to 3 days the cells appeared round and plump with only a few sites of local attachment to the polymer (Fig. 5(a)). From day 4 onwards, noticeable spreading with development of filipodia was observed at the fibrin glue PCL-CaP interphase and distinct attachment to the PCL-CaP scaffold

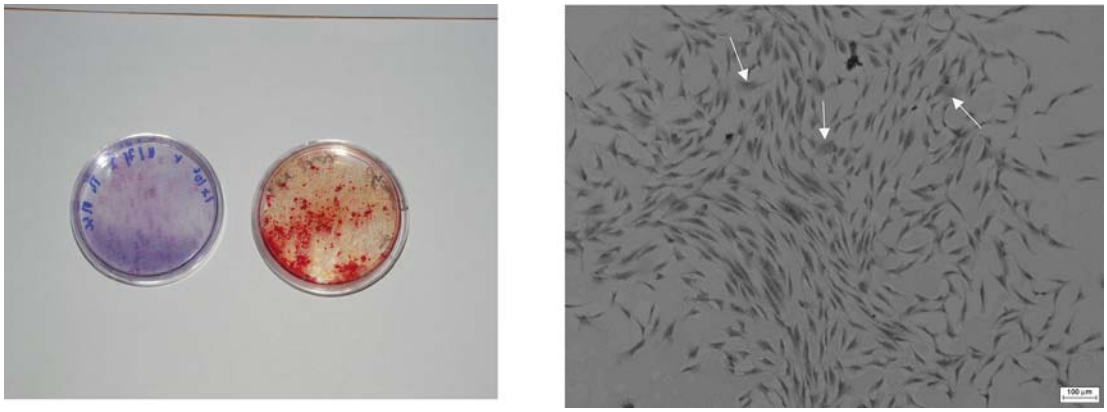

Figure 3 Fig. 3(a) shows a petri-dish cell culture plate containing human bone marrow derived mesenchymal stem cells colony forming units after 14 days of culturing. The cultures are fixed and stained with Wright's Giemsa. The colonies vary in size and are diffusely distributed in the dish. The number of colonies increased progressively during the culture period with a peak reached at day 14 after which only the size increased. Fig. 3(b) displays the details of a colony (original magnification $\times 10$). The typical morphology of spindle-shaped fibroblast like cells is the dominant phenotype of the cells in the colony. In between there are larger mononucleated polygonal shaped cells (arrows). Fig. 3(c) displays a culture stained with Alizarin-Red (pH 1) stain to verify that hMSC can undergo osteogenic differentiation. Multiple red foci indicating mineralised nodules.

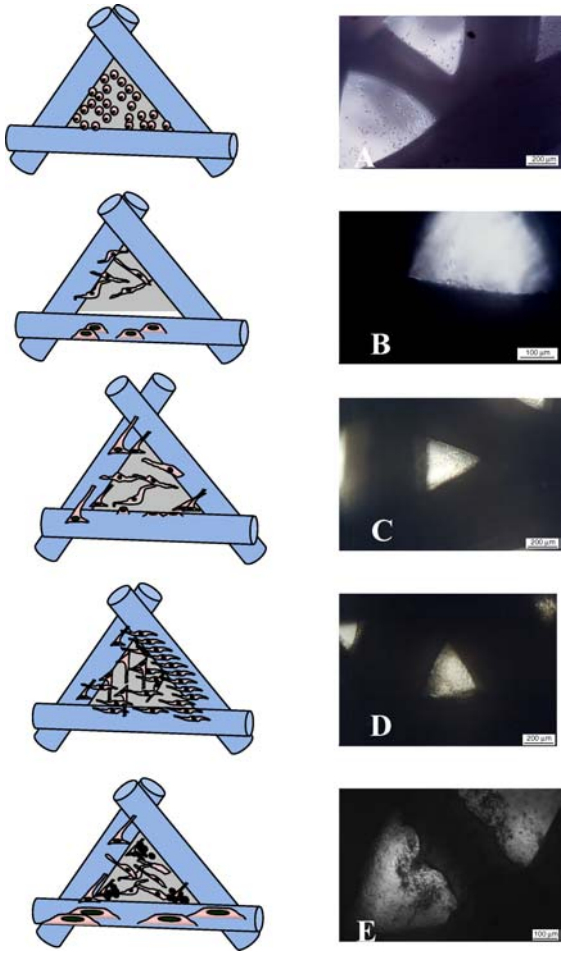

Figure 4 Analysis of cell attachment, proliferation and differentiation on the bars of the PCL-CaP scaffold. The left panel shows in a cartoon the sequence of 5 characteristic stages how the cells are colonizing the scaffold. The right panel depicts the corresponding light microscopy pictures of the different stages. In the first stage of cell adhesion the cells are predominantly round. This stage is followed by cell migration with spreading and the formation of cellular multilayers usually after 2–3 days in culture. In a third stage cellular bridging between adjacent bars occurs first in the corner of the pores. The fourth stage is characterized by the formation of a dense cellular network filling out the complete porous space of the scaffold and colonizing the bars and struts. In the final stage cells change from the proliferation to the differentiation stage characterized by matrix production and mineralization in the form of black clusters of nodules.

matrix occurred (Fig. 5(b)). The attached cells had a cuboidal appearance suggesting that the soft fibrin matrix wraps around the cells. When focal contact formation was present cytoskeletal organization was observed. The EYFP labeled microtubules which were diffusely distributed in round cells underwent reorganization in attached cells with distinct filaments stretching out from the microtubule organizing center along the axis of the cell (Fig. 5(a)). Within the pores cellular organization was observed and was characterized by circular, centripetally directed reformation. Cells in the angle of the scaffold develop multiple focal adhesions with long refractile cytoplasmic processes (Fig. 5(c)). The corresponding SEM image shows that cells anchored strongly to the PCL-CaP surface (Fig. 5(d)).

3.4.2. Analysis of cell proliferation and cellular organization with the scaffolds

Confocal laser microscopy of FDA labeled cells after 4 and 8 weeks demonstrated high densities of viable cells (Fig. 6(a) and (b)), confirming the results from the MTS assay shown in Fig. 6(f). However a slight increase of dead cells (stained red with Propidium Iodide) were present after 8 weeks in culture (Fig. 6(b)). It is possible, that the cell death was triggered by cell contact growth inhibition, because multiple layers were observed. The MTS mitochondrial activity showed a moderate early proliferation of about one population doubling, followed by a more gradual increase of approximately 50% over the remaining 42 days of the experiment (Fig. 6(c)).

3.4.3. Cell differentiation and assessment of mineralization and calcified nodule formation

The expression of extracellular osteocalcin after 4 weeks (Fig. 7), indicated the successful differentiation of the seeded MSCs into mature osteoblasts (Fig. 7(a)). Osteocalcin expression was found to be increased after

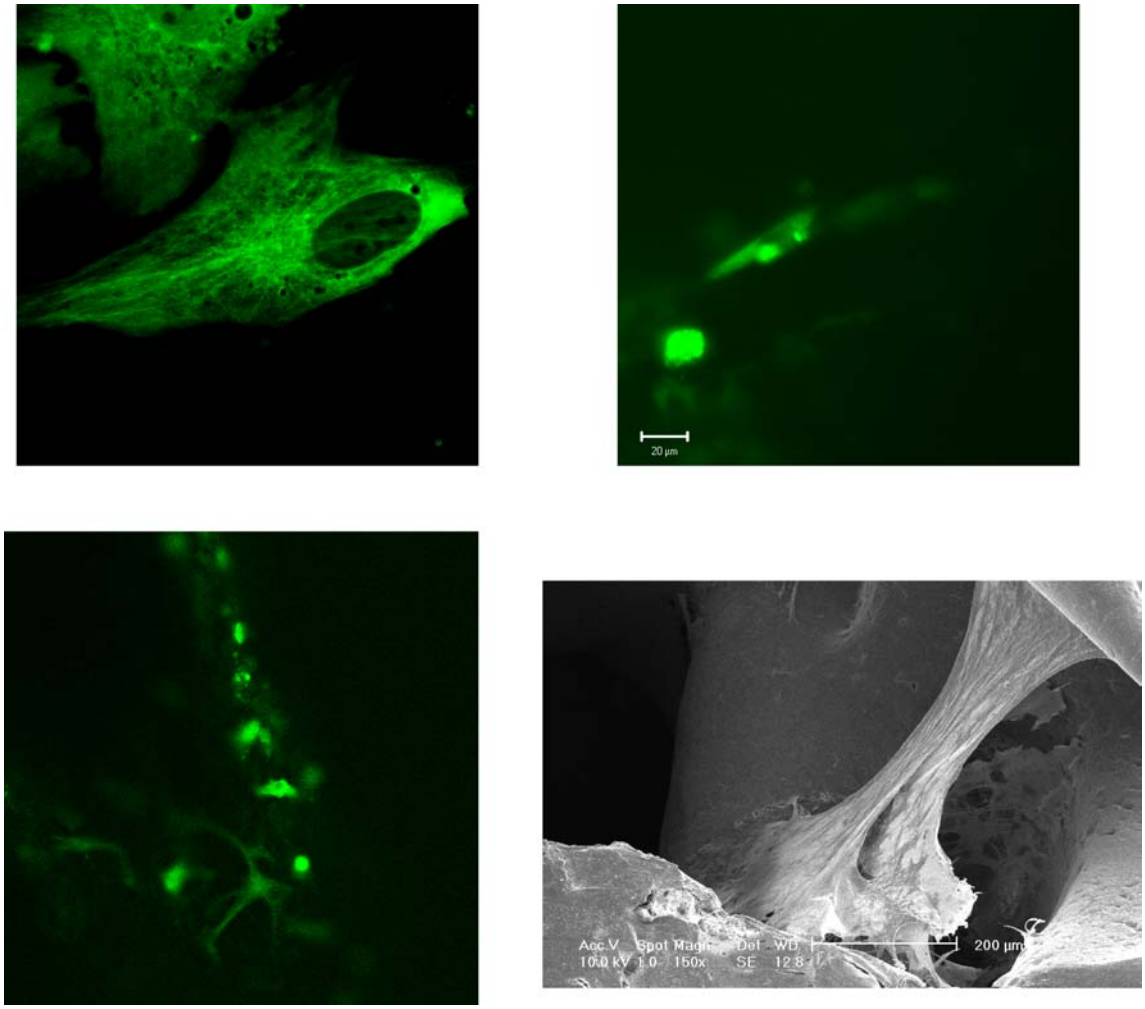

Figure 5 The formation of focal contacts of the seeded MPCs to the bars of the PCL-CaP scaffolds is visualized using confocal laser scanning microscopy and scanning electron microscopy. Fig. 5(a) shows a confocal laser microscopy image of a plated mesenchymal progenitor cell transfected with α-tubulin EYFP to label the microtubules. The cells were enzymatically detached 24 h after transfection and seeded in the scaffold. The seeded cells are initially rounded and the cytoskeleton is unorganized (Fig. 5(b) original magnification $\times$20). After 8 h post seeding significant cell spreading occurred. The formation of focal contact sites can be observed in Fig. 5(c) (original magnification $\times$10). The attached cells colonized on the PCL-CaP bars like roots of a tree with the irregular scaffold surface providing ideal anchoring spots for the cells as seen in the scanning electron microscopy (Fig. 5(d) original magnification $\times$150).

8 weeks (Fig. 7(b)). Detailed SEM examination demonstrated that the embedded cells partially resorb the surrounding fibrin glue matrix in a halo fashion and subsequently start forming new ECM (Fig. 8(a) after 4 weeks and Fig. 8(b) after 8 weeks). An increase in mineralized matrix deposits after 8 weeks is noticed in the cultured samples when compared to specimen 4 weeks in culture. In the SEM, a fibrilar network with matrix vesicles and nodules was visible. Immunohistochemical staining revealed that cells and nodules were embedded within a collagen I rich extracellular matrix (Fig. 9).

3.4.4. Assessment of mineralisation by surface analysis

Assessment of the matrix mineralization via EDAX (Fig. 10(a)–(d)) and alizarin complexone staining (Fig. 11(a) and (b)) showed a significant increase in Calcium and Phosphorus deposition between 4 to 8 weeks ($p \leq 0.5$). Nodule formation first occurred near the corners of the pores and close to the bars and struts and subsequently filled the pore volume with a dense layer at week 8. Note that the scaffold bars are strongly stained by alizarin complexone owing to the presence of the CaP component.

4. Discussion

Caplan and coworkers were among the first to study the potential of MSC in bone tissue engineering by using a scaffold in combination with human MSC [29–30]. A number of groups followed by using different types of scaffolds made of either synthetic polymers, natural polymers or ceramics (for review see Hutmacher [1]). The so called first generation type of scaffolds illustrated the potential to culture osteogenic scaffold/cell constructs but showed at the same time room for improvement from a matrix material point of view.

The osteoconductive properties of calcium phosphate (CaP) when incorporated into polymer composites has stimulated research into polymer/ceramic blends and ceramic coatings on polymer matrices for bone tissue engineering applications.

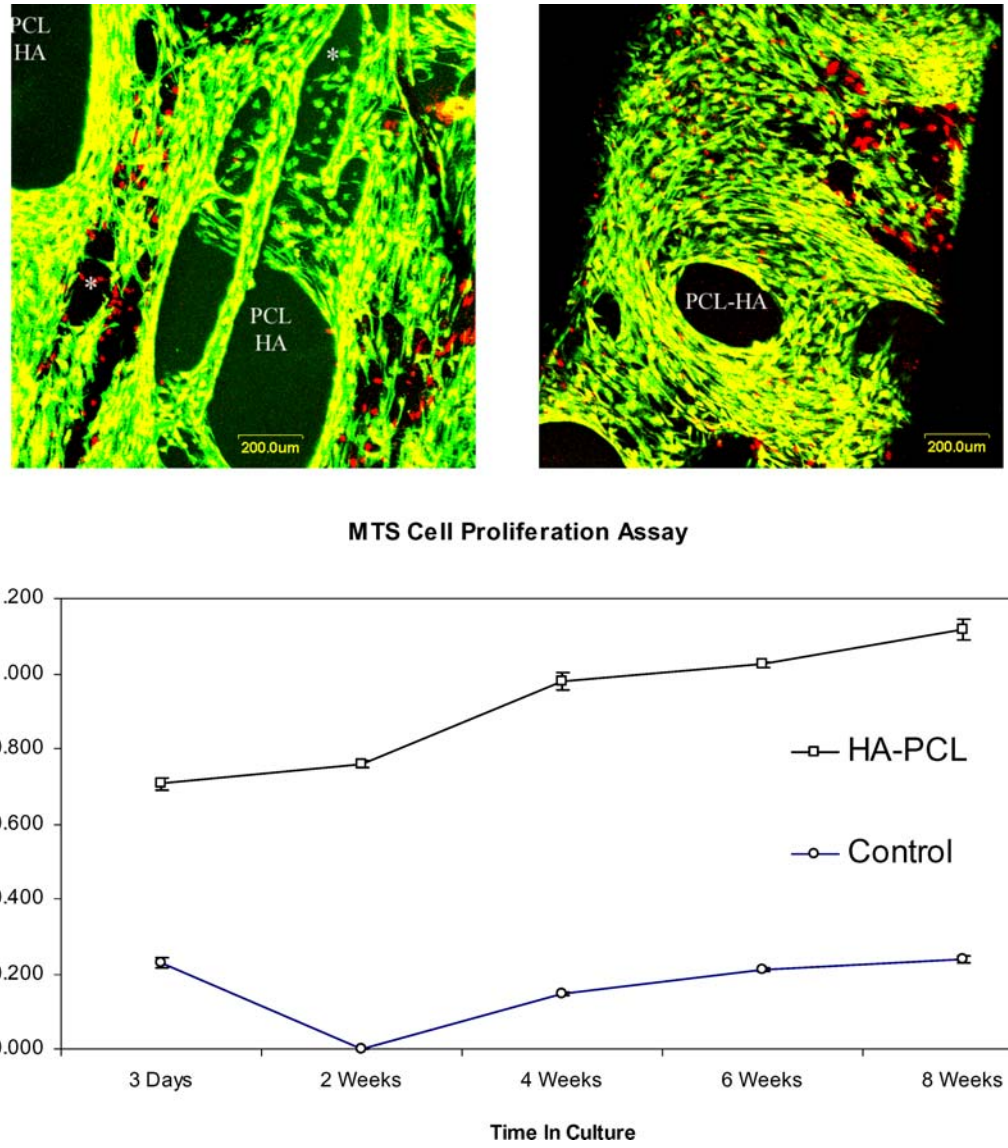

Figure 6 Characterization of cell proliferation and viability on the PCL-CaP scaffold. Viable cells are stained with fluorescence diacetate (FDA, green stain), while nuclei of apoptotic cells and cytoplasm of dead cells are counterstained with propidium iodide (PI, red stain). Optical sectioning was performed with a confocal laser microscope and superimposed images are shown (both original magnification $\times 10$). A dense cellular network can be observed after 4 weeks in culture (Fig. 6(a)), covering the bars and struts of the scaffold with only a few spaces in the pores left open (stars). After 8 weeks the remaining spaces are filled up completely. A slight increase in non-viable and apoptotic cells (red) is noticed (Fig. 6(b)). Fig. 6(c) shows a semi-quantitative MTS analysis of cell proliferation. Values represent the mean $\pm$ SD of five readings. The first stage is the proliferation phase were the cells multiply within the fibrin gel. The MTS graph indicates a steady increase in cell proliferation over the 8 weeks of culture.

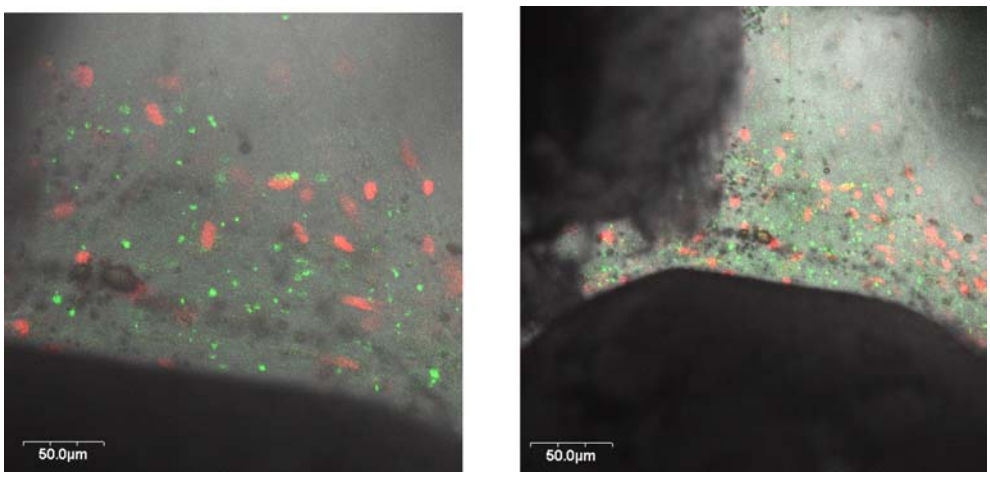

Figure 7 Osteocalcin expression in the cell-seeded PCL-CaP scaffolds after 4 (Fig. 7(a)) and after 8 weeks (Fig. 7(b)) in culture. The bone specific marker osteocalcin (green staining) confirms the presence of differentiated osteogenic cells. The cell nuclei were counter-stained with propidium iodide (red staining) and pictures are superimposed with transmitted light images for identifying scaffold pore and bar areas. There is an increase in osteocalcin production after 8 weeks (Fig. 7(b)).

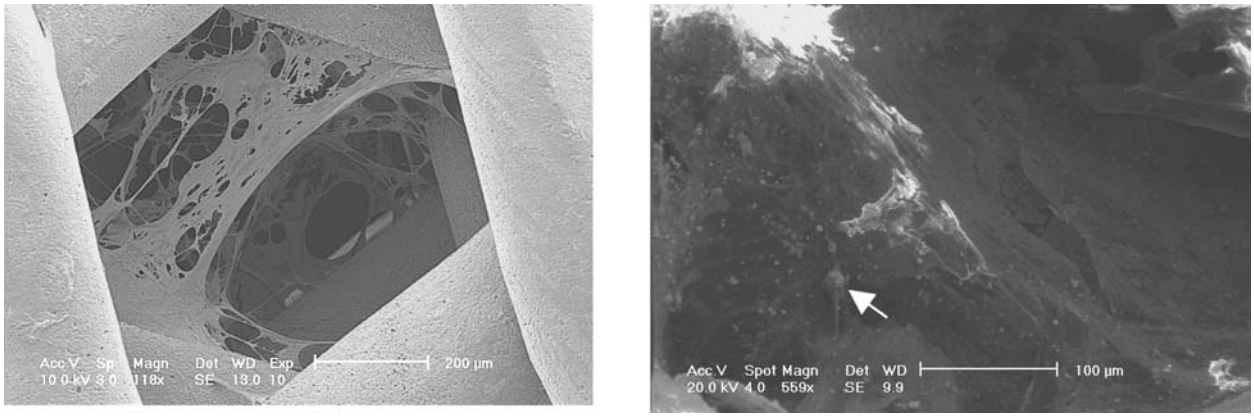

Figure 8 SEM micrographs of the cell seeded PCL-CaP scaffolds after 4 weeks (Fig. 8(a), original magnification ×118) and 8 weeks (Fig. 8(b), original magnification ×559) in culture. After 4 weeks dense colonization of the pores and bars of the scaffolds is present. The cells have a polygonal shape and are surrounded by the remaining fibrin glue and freshly produced extracellular matrix (ECM). Note the absence of mineralized nodules. After 8 weeks a significant increase in ECM production is observed with the cells being embedded in a fibrillar network of nodules in different stages of calcification (arrow).

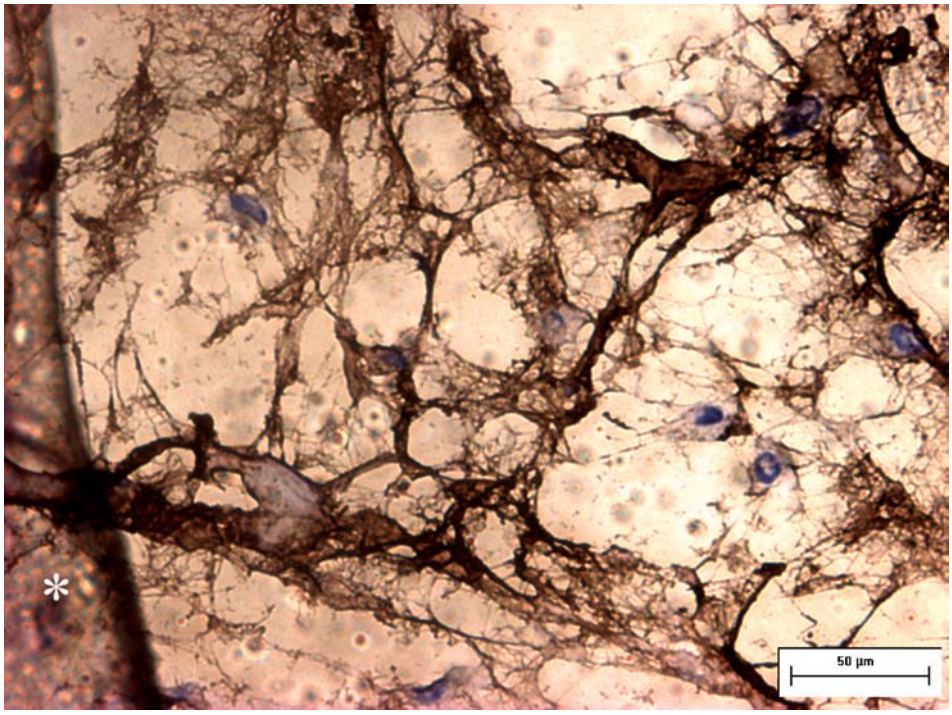

Figure 9 Photomicrograph showing a cryostat section of a cell-seeded PCL-CaP scaffold after 8 weeks in culture (original magnification ×10). The section was immunohistochemically stained for type I collagen (brown/black). The nuclei have been counterstained with Meyer's hematoxylin (blue). The pores are filled with a strongly stained collagen-rich matrix indicating the *in vitro* osteogenesis. The bar of the composite scaffold is marked with a star.

Hydroxyapatite/poly(L)lactide (HA/PLLA) blends have been made by melting and hot/cold pressing ([9, 31] solvent casting [44] and *in situ* polymerization [32, 33] prepared foam-like scaffolds of PLLA and PLLA/HA composites using solid/liquid phase separation. Their results revealed that polymer scaffolds supported cell growth only on the exterior of the matrix whereas more cells became attached throughout the architecture of composite scaffolds. In contrast, Marra *et al.* [34] studied foam like scaffolds of PCL, PGLA and PCL/HA and PGLA/HA composites manufactured by NaCl particle leaching. Formation of a thick cell sheet on the outside of all scaffold compositions was reported but only limited cell ingress and collagen deposition throughout 1 mm thick HA/polymer composite scaffolds. It is likely that the lower level of ingress and attachment observed was a function of the much lower and narrower interconnectivity produced by solvent leaching techniques.

Most conventional polymer processing techniques have the disadvantage that the compounded ceramic particulate tends to be separated from direct cell contact by a skin of polymer at the matrix surface. Such composites also generally show poor binding to the polymer matrix which results in insufficient mechanical property requirements for load-bearing hard tissue repair. Most importantly, traditional compounding and composite manufacturing routes do not allow fabrications of scaffolds layer by layer to vary the design and function of the different materials in one scaffold. In

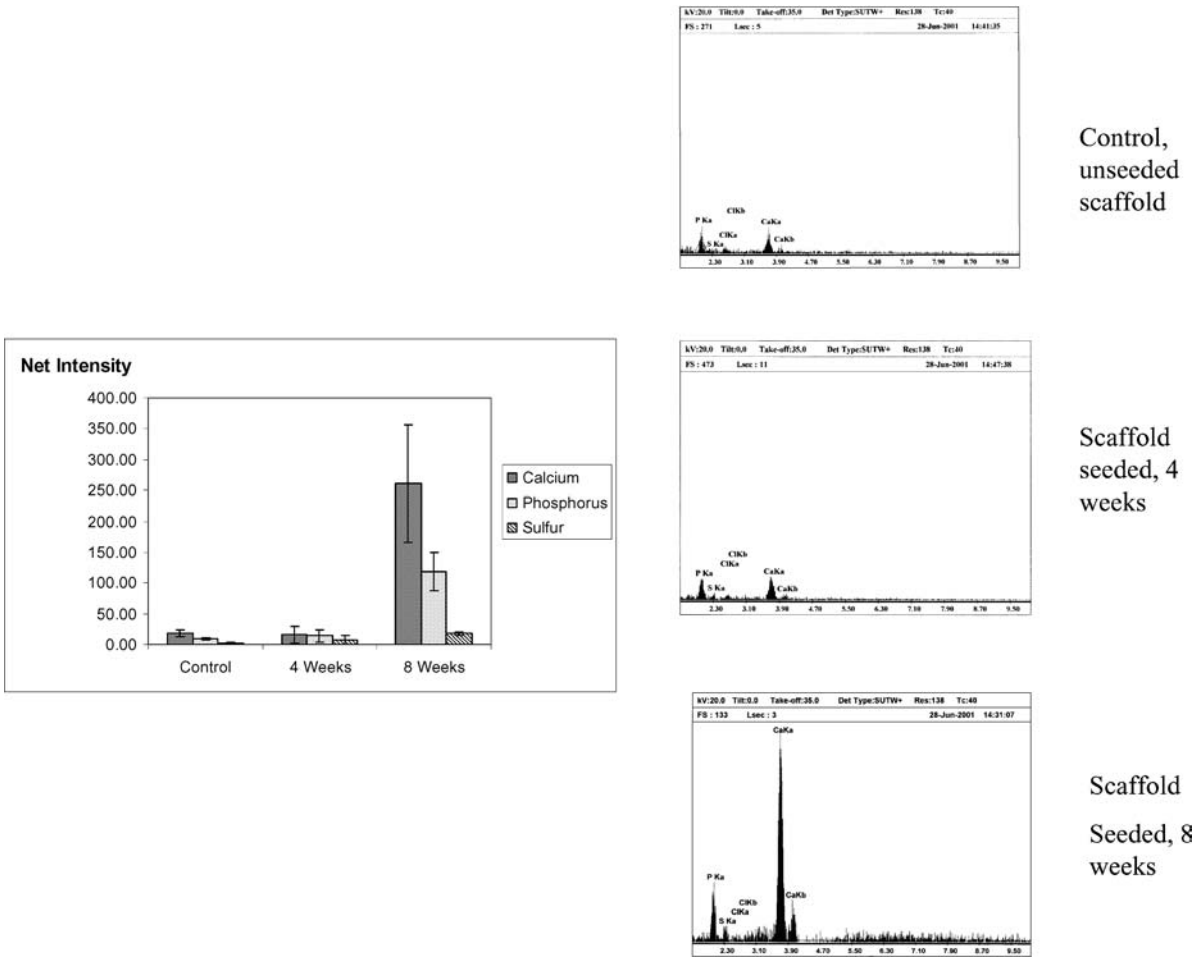

Figure 10 Assessment of mineralization by EDAX surface analysis. The EDAX spectrum of the 8 weeks specimens shows prominent peaks for Ca and P (Fig. 8(d)) when compared to the 4 weeks group (Fig. 8(c)). This demonstrates the presence of a mineral phase rich in calcium (Ca) and phosphorus (P). Linked to the presence of cells and the extracellular organic matrix was the presence of chlorine (Cl) and sulphur (S) peaks, probably due to the synthesis of sulphated proteoglycans by the cells. The spectrum of an unseeded PCL-CaP scaffold is shown in Fig. 9(c) as a material reference respectively. The corresponding graph (Fig. 8(e)) confirms the significant increase ($p < 0.05$) of Ca and P deposition after 8 weeks.

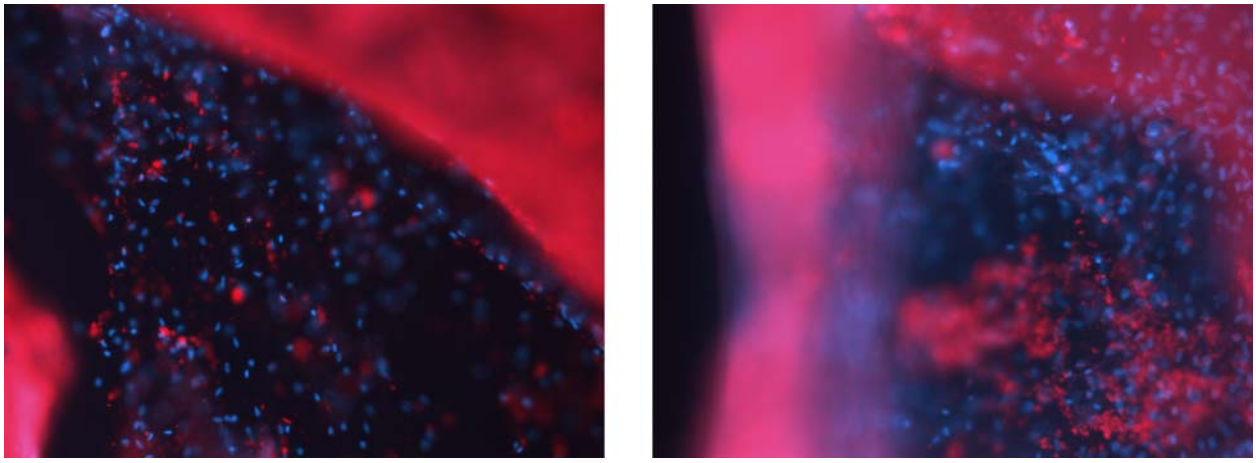

Figure 11 Conventional fluorescence microscopy of a cell-biomaterial section stained with alizarine-complexone and nuclear counterstaining using DAPI. The bars of the PCL-CaP scaffolds are stained red indicating the Ca component of the hydroxyapatite. Fig. 11(a) shows the presence of a mineralized nodule after 4 weeks in culture. A significant increase in calcium deposition is noticed after 8 weeks (Fig. 11(b)). Diffusely arranged nodules (red staining) have filled up the pores of the scaffold architecture.

contrast, SFF and indirect SFF provide the ability to create internal architecture of biomimetic structures of various designs and material compositions, a freedom to design global pore structure in 3D space (interconnectivity, branching, geometry, diameter, and orientation) and precise control over scaffold external geometry to match the implant site. Generally, these techniques provide enhanced control over scaffold physical and chemical properties, bioactivity, and degradation kinetics [6].

We have developed PCL/CaP composites by using FDM as manufacturing technique. Data of this study

show calcium phosphate particles are distributed in the matrix and at the same time exposed on the surface after short NaOH treatment. Contact angle shows that such composite surfaces are more hydrophilic and that the degradation kinetics are 3 to 4 times accelerated compared to PCL alone. Ural *et al.* [35] studied copolymers of PCL/PDLA and PCL/PDLA/CaP blends and conclude that the CaP component leads to faster degradation kinetics. These findings were confirmed by Marra *et al.* [34]. who showed that addition of CaP to CaP/PCL/PLGA blends increased degradation rate and CaP dominated degradation at higher volume fractions with no significant difference between different polymer blends.

Rizzi *et al.* [18] in studies of simple PLA/HA and PCL/HA mixtures prepared by solvent casting onto glass surfaces showed that cells tended to attach to and bridge between surface-exposed HA particles and that the presence of HA led to increased cell activity. It was concluded that the presence of exposed HA may provide a means for control of cell density on material surfaces. However it is difficult to extrapolate the findings from these studies of 2D preparations to the likely behavior of 3D scaffolds.

For scaffolds with a much lower volume/surface area ratio such as textile preparations [36–37] and the FDM scaffolds with a honey-comb and channel-like architecture reported here a different problem arises. From a physical point of view the low surface areas available for cell attachment reduces volumetric seeding efficiency when using conventional pippeting methods. A means of overcoming this deficiency is to deliver and support the cells in a gel matrix which retains the cells within the interstices of the scaffold. Several groups have developed methods of entrapping cells in various hydrogels including fibrin glue [27], alginate [38], collagen [39] and agarose [36] which are subsequently injected into a variety of synthetic scaffold types.

A number of investigators have favored fibrin glue as a cell support in order to take advantage of additional benefits conferred by fibrin and other proteins and biomolecules such as fibronectin present within the fibrin glue preparations. Several of these proteins have been shown to have important roles in wound healing and osteogenesis. For example fibronectin plays a major role in early osteogenesis [40] by supporting the migration and proliferation of undifferentiated MSCs within the stabilized fibrin network.

The data presented in this study shows that mesenchymal progenitor cells migrate effectively into and through the fibrin glue. The hydrogel matrix allows the cells to proliferate without deforming cell structure and supports cellular attachment to the rigid polymer structures in the initial phase. Furthermore the hydrogel accommodates factors affecting osteogenic cell differentiation. Hence fibrin glue is an appropriate delivery substance for inoculating cells into 3D scaffold systems.

ECM matrix composition in the "cell-seeded" PCL-CaP was therefore analyzed using immunohistochemistry. The staining showed that collagen I fibrils are widely present in the matrix (Fig. 8). This observation represents further evidence that early bone formation occurred.

The biomineralisation of the extra cellular matrix during culturing Scaffold/cell constructs represents an essential criterion in bone engineering. When osteoblast-like cell populations are maintained for extended periods in the presence of serum and ascorbate, cell proliferation continues post-confluence in foci scattered throughout the monolayer. When culturing is continued these foci develop into well-defined three-dimensional adherent cell arrays termed "bone-nodules". The nodules have a thickness of 50–100 μm and consist of approximately 100 cells surrounded by a collagen rich extracellular substratum of numerous vesicular structures. The localized pilling of confluent cells into "bone nodules" characterizes a late stage of osteoblast differentiation [41] and is essential for *in vitro* formation of human bone [42]. The results from the EDAX X-ray diffraction analysis showed that the mineral phase is comprised of poorly crystalline hydroxyapatite (Fig. 9). It has been previously described that these nodules represent the *in vitro* onset of bone formation [41].

Scanning electron microscopy was employed to visualize the cell-material interphase and in combination with the SEM-EDAX to assess the surface morphology and elemental characteristics of the composite material and tissue formation. It has been shown by many investigators that surface topography affects the cell/material interaction and subsequently the function of the cell in terms of proliferation and differentiation. We observed that cells preferentially adhere to the corners of the pores and struts and stretch between closely positioned bars. SEM as well as inverted light microscopy analysis indicates that in these areas cellular differentiation occurred first with the onset of mineralized nodule formation, being observed after 4 weeks. It is proposed that the surface characteristics and scaffold architecture induce mechanical stress on the cell, which are transmitted over the cytoskeleton and lead to conformational and biochemical changes in the cell metabolism.

In the presented EDAX spectrum Ca and P peaks were prominent and reach a maximum after 8 weeks. The detected Ca and P in the control group confirm the presence of CaP particles in the polymer. Other elements recorded in the spectra such as sulphur and chlorine were due to the buffer salts used for the cell culture. Alizarin complexone staining, a calcium specific fluorescent stain (Fig. 10) confirmed the presence of multiple mineralized nodules, which is a good index of osteogenesis *in vitro* [43]. It was shown that there is a significant increase in positively stained nodules within the pores after 8 weeks compared to 4 weeks. This is in concordance with EDAX analysis of the mineralized phase.

5. Conclusion

Bone development requires the concerted action of several micro-environmental signals: cell-cell interaction, cell-ECM interaction and cell-biomaterial interaction. Hence, an essential component in the differentiation

and subsequent mineralization of progenitor cells is the design and the composition of the scaffold matrix on which cells are seeded. This *in vitro* study provided histological and biochemical evidence that the combination of PCL-CaP scaffolds seeded with bone marrow derived MSCs using fibrin glue leads to proliferation within the scaffold and differentiation of the cells along the osteogenic lineage. The PCL-CaP scaffold represents a physically stable and bioactive framework for bone formation. Whereas the fibrin glue acts as an effective cell delivery vehicle and provides a biomimetic microenvironment suitable for cell proliferation and differentiation.

Acknowledgments

The authors thank Ms Conny Er from the Clinical Research Center, National University of Singapore for the excellent technical assistance with the Immunocytochemistry and the Confocal images. Dr. Robert E. Guldberg, Georgia Tech Emory Center is thanked for the micro-CT analysis of the PCL-CaP scaffolds. Prof Teoh Swee Hin, Department of Mechanical Engineering and Graduate Program in Biomedical Engineering, National University of Singapore and Mr. Tan Kim Cheng, School of Engineering, Temasek Polytechnic Singapore, are thanked for assisting in the fabrication of the PCL-CaP scaffolds. This study was supported by the National University of Singapore Young Investigators Award WBS No. R-397 000 003 650.

References

1. D. W. HUTMACHER, *Biomaterials* **21** (2000) 2529.
2. D. GREEN, D. WALSH, S. MANN and R.O. OREFFO, *Bone* **30** (2002) 810.
3. C. M. AGRAWAL and R. B. RAY, *J. Biomed Mater. Res.* **55** (2001) 141.
4. H. SHIN, S. JO and A. G. MIKOS, *Biomaterials* **24** (2003) 4353.
5. D. W HUTMACHER, T. SCHANTZ, I. ZEIN. K. W. NG, S. H. TEOH and K. C TAN *J. Biomed. Mater. Res.* **55** (2001) 203.
6. S. J. HOLLISTER, R. D. MADDOX and J. M TABOAS, *Biomaterials* **20** (2002) 4095.
7. H. AOKI, K. KATOH, T. TABATA and M. OGISO, *Shikai Tenbou* **49** (1987) 567.
8. I. ONO, T. OHURA and M. MURATA, *Plast. Reconstr. Surg.* **90** (1992) 870.
9. R. ZHANG and P. X. MA, *J. Biomed. Mater. Res.* **44** (1999) 446.
10. T. J. CORDEN, I. A. JONES, C. D. RUDD, P. CHRISTIAN, S. DOWNES and K. E. MCDOUGALL, *Biomaterials* **21** (2000) 713.
11. J. T. SCHANTZ, D. W. HUTMACHER, H. CHIM, K. W. NG, T. C. LIM and S. H. TEOH, *Cell Transpl.* **11** (2002) 125.
12. J. T. SCHANTZ, D. W. HUTMACHER, C. X. LAM, M. BRINKMANN, K. M. WONG, T. C. LIM, N. CHOU, R. E. GULDBERG and S. H. TEOH, *Tissue Eng.* **9** (Suppl 1) (2003) S127.
13. M. ENDRES, D. W. HUTMACHER, A. J. SALGADO, C. KAPS, J. RINGE, R. L. REIS, M. SITTINGER, A. BRANDWOOD and J. T. SCHANTZ, *ibid.* **9** (2003) 702.
14. H. OHGUSHI and M. OKUMURA, *Acta Orthop. Scand.* **61** (1990) 431.
15. H. OHGUSHI, Y. DOHI, S. TAMAI and S. TABATA, *J. Biomed. Mater. Res.* **27** (1993) 1401.
16. H. OHGUSHI and A. I. CAPLAN, *ibid.* **48** (1999) 913.
17. T. NOSHI, T. YOSHIKAWA, Y. DOHI, M. IKEUCHI, K. HORIUCHI, K. ICHIJIMA, M. SUGIMURA, K. YONEMASU and H. OHGUSHI, *Artif Org.* **25** (2001) 201.
18. S. C. RIZZI, D. J. HEATH, A. G. COOMBES, N. BOCK, M. TEXTOR and S. DOWNES, *J. Biomed. Mater. Res.* **15** (2001) 475.
19. S. J. PETER, P. KIM, A. W. YASKO, M. J. YASZEMSKI and A. G. MIKOS, *J. Biomed. Mater. Res.* **5** (1999) 314.
20. M. S. WOLFE, D. DEAN, J. E. CHEN, J. P. FISHER, S. HAN, C. M. RIMNAC and A. G. MIKOS, *ibid.* **61** (2002) 159.
21. A. A. IGNATIUS, M. OHNMACHT, L. E. CLAES, J. KREIDLER and F. A. PALM, *J. Biomed. Mater. Res. (Appl. Biomater.)* **58** (2001) 564.
22. A. JOHN, L. HONG, Y. IKADA and Y. TABATA, *J. Biomater. Sci. Polym. Ed.* **12** (2001) 689.
23. C. E. HOLY, M. S. SHOICHET and J. E. DAVIES, *J. Biomed. Mater. Res.* **51** (2000) 376.
24. J. L. DRURY and D. J. MOONEY, *Biomaterials*. **24** (2003) 4337.
25. J. T. SCHANTZ, D. W. HUTMACHER, A. M. CHOU, S. S. GOUK, T. G. PARK, R. L. REIS, T. C. LIM and S. H. TEOH, in Proceedings of the International Conference on Materials for Advanced Technologies, Singapore, July 1–6, 2001.
26. A. REDLICH, C. PERKA, O. SCHULTZ, R. SPITTER, T. HAUPL, G. R. BURMESTER and M. SITTINGER, *J. mater. Sci.: Mater. Med.* **10** (1999) 767.
27. N. ISOGAI, W. J. LANDIS, R. MORI, Y. GOTOH, L. C. GERSTENFELD, J. UPTON and J. P. VACANTI, *Plast Reconstr. Surg.* **105** (2000) 953.
28. A. S. LIN, T. H. BARROWS, S. H. CARTMELL and R. E. GULDBERG, *Biomaterials*. **24** (2003) 481.
29. S. E. HAYNESWORTH, M. A. BABER and S. I. CAPLAN, *Bone* **13** (1992) 81.
30. J. E. DENNIS, S. E. HAYNESWORTH, R. G. YOUNG and S. I. CAPLAN, *Cell Transpl.* **1** (1992) 23.
31. S. H. LI, J. R. DE WIJN, P. LAYROLLE and K. DE GROOT, *J. Biomed. Mater. Res.* **61** (2002) 109.
32. Q. ZHENG, X. GUO, J. DU and Y. LIU, *Chin. Med. Sci. J.* **16** (2001) 141.
33. P. X. MA, R. ZHANG, G. XIAO and R. FRANCESCHI, *J. Biomed. Mater. Res.* **54** (2001) 284.
34. K. G. MARRA, J. W. SZEM, P. N. KUMTA, P. A. DIMILLA and L. E. WEISS, *J. Biomed. Mater. Res.* **47** (1999) 324.
35. E. URAL, K. KESENCI, L. FAMBRI, C. MIGLIARESI and E. PISKIN, *Biomaterials*. **21** (2000) 2147.
36. N. ROTTER, J. AIGNER, A. NAUMANN, H. PLANCK, C. HAMMER, G. BURMESTER and M. SITTINGER, *J. Biomed. Mater. Res.* **42** (1998) 347.
37. L. E. FREED, G. VUNJAK-NOVAKOVIC, R. J. BIRON, D. B. EAGLES, D. C. LESNOY, S. K. BARLOW and R. LANGER, *Biotechnology* (NY) **12** (1994) 689.
38. S. C. CHANG, G. TOBIAS, S. K. ROY, C. A. VACANTI and L. J. BONASSAR, *Plast Reconstr Surg.* **112** (2003) 793.
39. G. CHEN, T. SATO, T. USHIDA, R. HIROCHIKA and T. TATEISHI, *FEBS Lett.* **8** (2003) 95.
40. J. WANG, R. YANG, L. C. GERSTENFELD and M. J. GLIMCHER, *Calcif Tissue Int.* **67** (2000) 314.
41. J. N. BERESFORD, S. E. GRAVES and C. A. SMOOTHY, *Amer. J. Med. Genet* **45** (1993) 163.
42. S. KALE, S. BIERMANN, C. EDWARDS, C. TARNOWSKI, M. MORRIS and M. W. LONG, *Nat Biotechnol.* **18** (2000) 954.
43. I. D. XYNOS, M. V. J. HUKKANEN, J. J. BATTEN, L. D. BUTTERY, L. L. HENCH and J. M. POLAK, *Calcif Tissue Int.* **67** (2000)321.
44. H. R. RAMAY and M. ZHANG, *Biomaterials* **24** (2003) 3293.

Received 5 February
and accepted 30 June 2004